INTERNATIONAL ATOMIC ENERGY AGENCY
UNITED NATIONS EDUCATIONAL, SCIENTIFIC AND CULTURAL ORGANIZATION

INTERNATIONAL CENTRE FOR THEORETICAL PHYSICS
34100 TRIESTE (ITALY) - P.O.B. 586 - MIRAMARE - STRADA COSTIERA 11 - TELEPHONE: 2240-1
CABLE: CENTRATOM - TELEX 460392-I

SMR/455 - 17

EXPERIMENTAL WORKSHOP ON HIGH TEMPERATURE SUPERCONDUCTORS & RELATED MATERIALS (BASIC ACTIVITIES)

12 - 30 MARCH 1990

CRITICAL CURRENTS

RENE FLÜKIGER

Kernforschungszentrum Karlsruhe
Institut Für Technische Physik
7514 Eggenstein-Leopoldshaften
Karlsruhe 7500
Federal Republic of Germany

INTRODUCTION

I. FUNDAMENTAL PROPERTIES

1. ZERO RESISTANCE

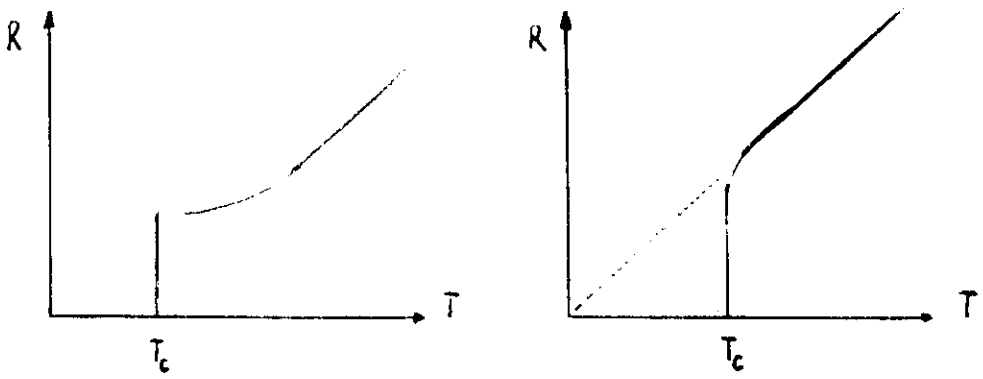

CONVENTIONAL SC [Clean] — HIGH-T_c SC [Clean]

$\rho(300\,K) \approx 1 - 10\ \mu\Omega cm$ — $\rho_{ab}(100\,K) \approx 50 - 60\ \mu\Omega cm$

- Normal State : Origin of R (conventional SC)
  - Scattering of e^- by phonons
  - Scattering of e^- by impurities

  } UNCORRELATED MOTION OF ELECTRONS

- SC State : $R = 0$ REQUIRES HIGHLY "ORGANIZED" MOTION OF "SC carriers" [Scattering of 1 "carrier" would imply simultaneous Scattering of $\sim 10^{23}$ "carriers" ⟹ EXTREMELY UNLIKELY]

⟹ All "SC CARRIERS" IN THE SAME QUANTUM STATE

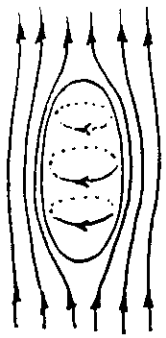

- Magnetic Field screened by supercurrents flowing at the surface of SC [⟹ Penetration Depth $\lambda \sim 500 - 5000\ \text{Å}$]
- SC (screening currents) supply work against magnetic pressure to keep Field out:

Energy cost / Unit Vol. $= -\frac{1}{2} MH = \frac{H^2}{8\pi}$
[long Cylinder $\parallel \vec{H}$]

- ⟹ Upper Field Limit for occurrence of SC : THERMODYNAMIC CRITICAL FIELD $H_c(T)$

g : Gibbs free Energy Density

SC-Phase : $g_{SH} = g_{SO} + \frac{H^2}{8\pi}$

N-Phase : $g_{NH} = g_{NO}$

SC-N Phase Transition [COEXISTENCE] : $g_{SH_c} = g_{NH_c}$

⟹ $\boxed{g_{NO} - g_{SO} = \frac{H_c^2(T)}{8\pi}}$ CONDENSATION ENERGY

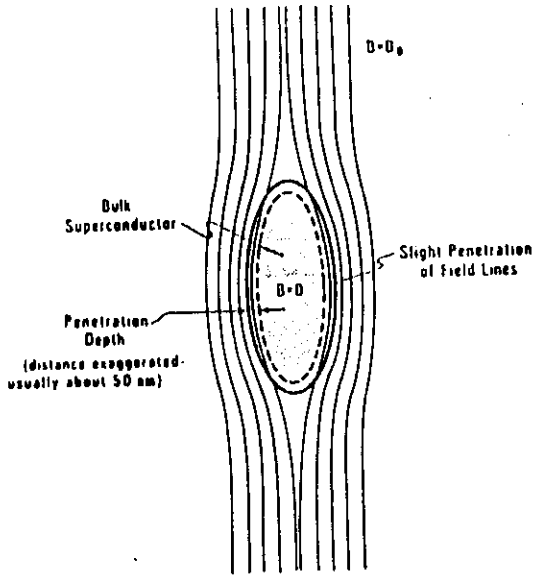

ılsion of flux from the interior of an ideal superconductor. Dashed shows the field penetration depth, λ, t the surface (not to scale) ɾell and Clark, 1977).

- Temperature Dependence of H_c : nearly Parabolic

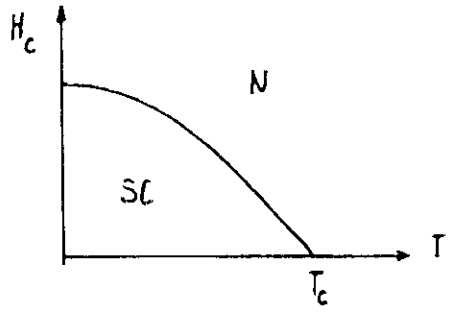

$$H_c(T) \approx H_c(0)\left[1-\left(\frac{T}{T_c}\right)^2\right]$$

	T_c (K)	$H_c(0)$ [kG]
Al	1.18	0.105
Nb	9.25	2.06
YBaCuO	95	~ 5

- Connection with Microscopic Theory (BCS) :

Condensation Energy is associated with Opening of an Energy GAP in Spectrum of electronic EXCITATIONS

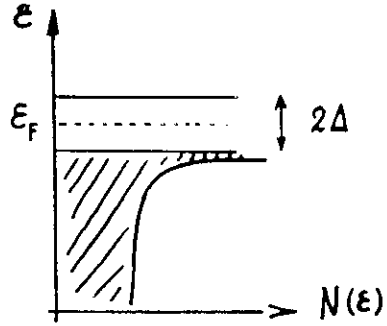

T=0 //// Filled STATES

Only FRACTION ~ $2\Delta/\varepsilon_F$ of ELECTRONS PARTICIPATES TO CONDENSATION PHENOMENON :

$$\frac{H_c^2(0)}{8\pi} \sim n\,\frac{2\Delta}{\varepsilon_F}\,2\Delta \sim N(\varepsilon_F)\,\Delta^2$$

$N(\varepsilon_F)$: Density of States at ε_F

III. PAIRING - COHERENCE LENGTH

- REQUIREMENT FOR SC : All "SC CARRIERS" IN THE SAME QUANTUM STATE

- NATURE OF "SC CARRIERS" ?

  - NOT SINGLE ELECTRONS (PAULI EXCLUSION PRINCIPLE)

  ⟹ CREATE "BOSONS" BY FORMING BOUND PAIRS OF ELECTRONS (COOPER PAIRS, 1956)

- MECHANISM FOR COOPER PAIR FORMATION IN "CONVENTIONAL" SC:

  ELECTRON - PHONON INTERACTION

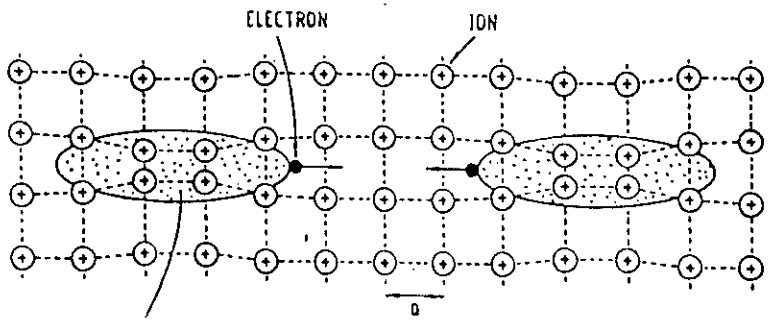

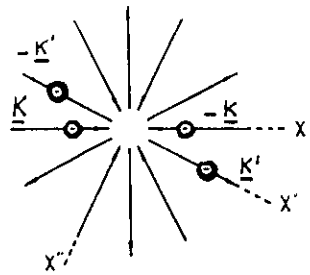

MOUVEMENT DES DEUX ELECTRONS DANS UNE PAIRE DE COOPER

S - STATE FOR SINGLET (↑↓) PAIRING

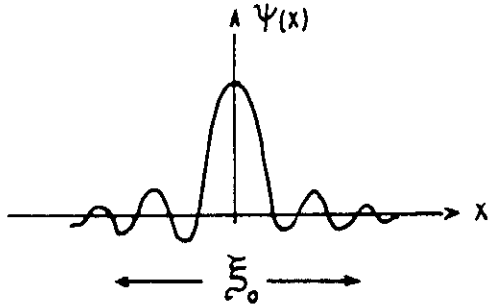

ξ_0 : COHERENCE LENGTH (SIZE OF COOPER PAIR)

PIPPARD, 1953

ESTIMATE OF ξ_0 :

- Only ELECTRONS WITH ENERGIES WITHIN 2Δ OF $\mathcal{E}_F$ PARTICIPATE TO PAIRING

- CHARACTERISTIC TIME FOR ELECTRON MOTION WITHIN A PAIR :

$$\tau \sim \frac{\hbar}{2\Delta} \quad \Rightarrow \quad \xi_0 \approx v_F \tau \approx \frac{\hbar v_F}{2\Delta}$$

Notice : $2\Delta \sim k_B T_c$ $\qquad v_F \sim n^{1/3}$

CONVENTIONAL SC : $n \sim 10^{23}$ el./

HIGH-T_c SC : $n \sim 10^{21}$ el./cm

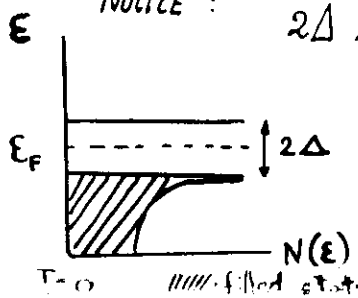

	Al (1.18 K)	Nb (9.25 K)	YBCO (95 K)	
ξ_0 [Å]	16'000	380	34	(a,b)
			7	(c)

- MACROSCOPIC QUANTUM-MECHANICAL NATURE OF SC-STATE:

COOPER PAIRS CONDENSE IN THE SAME QUANTUM STATE ⇒

ALL PAIRS HAVE IDENTICAL MOTION DESCRIBED BY A "MACROSCOPIC WAVEFUNCTION"

$$\Psi(\vec{r}) = |\Psi(\vec{r})| e^{i\varphi(\vec{r})}$$

- $\Psi(\vec{r})$ DESCRIBES CENTER-OF-MASS MOTION OF COOPER PAIRS
- $|\Psi(\vec{r})|^2 = n_s^*(\vec{r})$: DENSITY OF COOPER PAIRS
- PAIRS HAVE THE SAME PHASE $\varphi(\vec{r})$ (important for MACROSCOPIC QUANTUM INTERFERENCE)
- Characteristic LENGTH SCALE FOR SPATIAL VARIATIONS OF $\Psi(\vec{r})$: GINZBURG-LANDAU (GL) COHERENCE LENGTH (related to but distinct from ξ_0)

PURE SC ($\xi_0 \ll \ell$) $\quad \xi(T) \sim \xi_0 (T_c - T)^{-1/2}$

DIRTY SC ($\xi_0 \gg \ell$) $\quad \xi(T) \sim (\xi_0 \ell)^{1/2} (T_c - T)^{-1/2}$

Coherence length: Characterization of the local extension of a perturbation of $\Psi(x)$

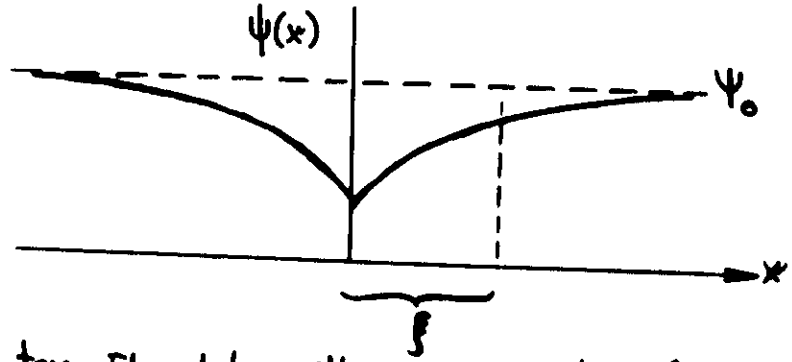

Vortex: Flux tube with the quantum flux $\Phi_0 = 2.07 \times 10^{-7}$ G cm²
The core is normal conducting ($\Psi = 0$, $B = \max$).

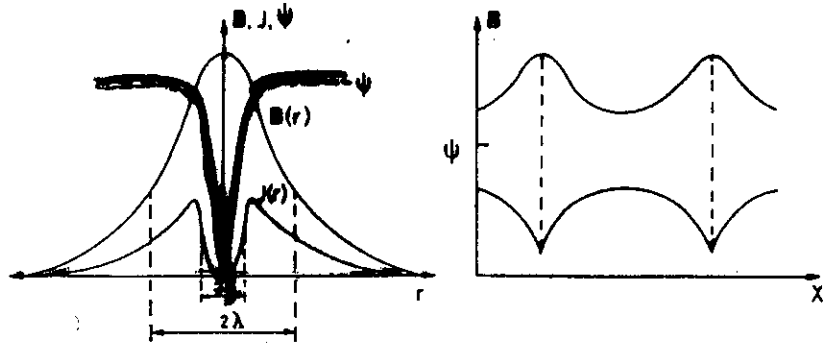

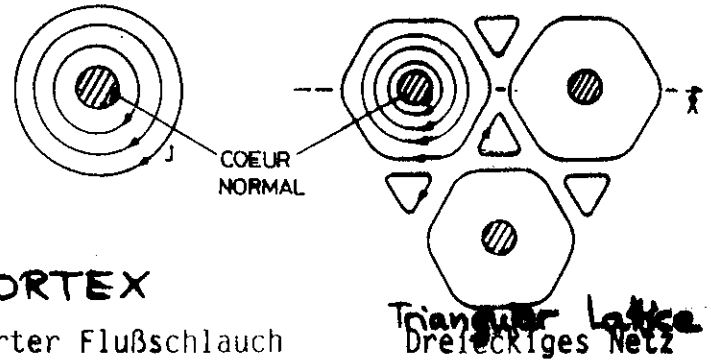

VORTEX

Isolierter Flußschlauch

Triangular Lattice

Dreieckiges Netz

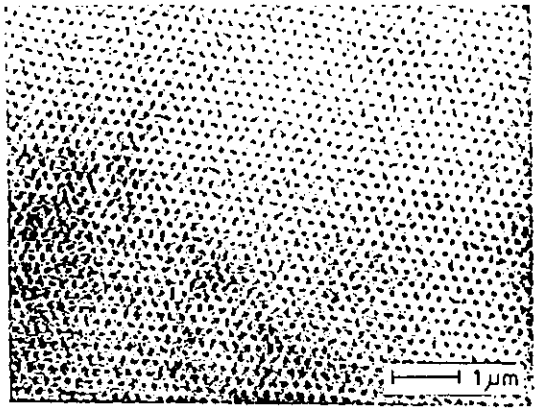

Fig.4.2. Triangular vortex lattice in a Nb disk (thickness = 0.5 mm; diameter = 4 mm) in a perpendicular magnetic field of 985 G at 1.2 K. The experimental observation utilizes a high-resolution Bitter method. (Courtesy of U. Essmann)

H.F. Hess et al.
Phys. Rev. Lett. 62, 214 (1989)

STM-PICTURE

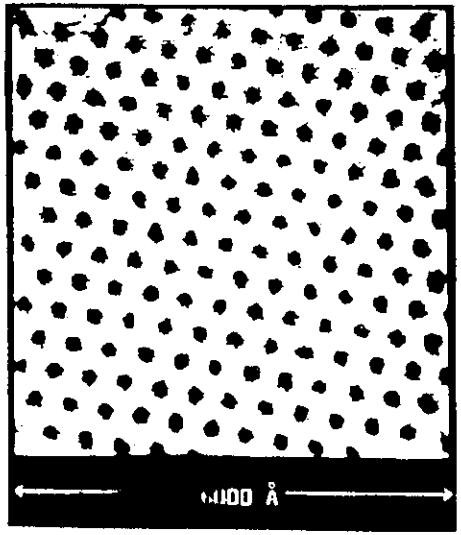

FIG. 2. Abrikosov flux lattice produced by a 1-T mag field in $NbSe_2$ at 1.8 K. The scan range is about 6000 Å. gray scale corresponds to dI/dV ranging from approxim 1×10^{-8} mho (black) to 1.5×10^{-9} mho (white).

System	T_c (K)	$\xi(0)$ (nm)	Reference
Nb_3Sn	18	7.5	Orlando et a
NbTi	9	4.3	Hake et al.
$PbMo_6S_8$	14.8	2.7	Foner et al.
$YBa_2Cu_3O_7$	90	2 - 3 ∥ 0.5 - 0.7 ⊥	Umezawa et a
$YBa_2Cu_3O_7$(film)	87	1.6 ∥ 0.2 ⊥	Oh et al. (2
$Bi_2Sr_2Ca_1Cu_2O_8$	84	3.1 ∥ 0.4 ⊥	Palstra et al
$Bi_2Sr_2Ca_1Cu_2O_8$	110	2.9 ∥	Yoshitake et
$Tl_2Ba_2Ca_2Cu_3O_8$	105	1.6 ∥	Kumakura et a

Tabelle I. Supraleitender Sprungpunkt T_c und Kohärenzlänge $\xi(0$

- Estimate of H_{c2} : N-State ∴ overlapping vortex

  CORES : $a \approx \xi \longrightarrow H_{c2} \approx \frac{\phi_0}{\xi^2}$

  Exact GL Result : $H_{c2} = \frac{\phi_0}{2\pi\xi^2} \sim (1-t)^2$

Applications !

- Vortex line structure

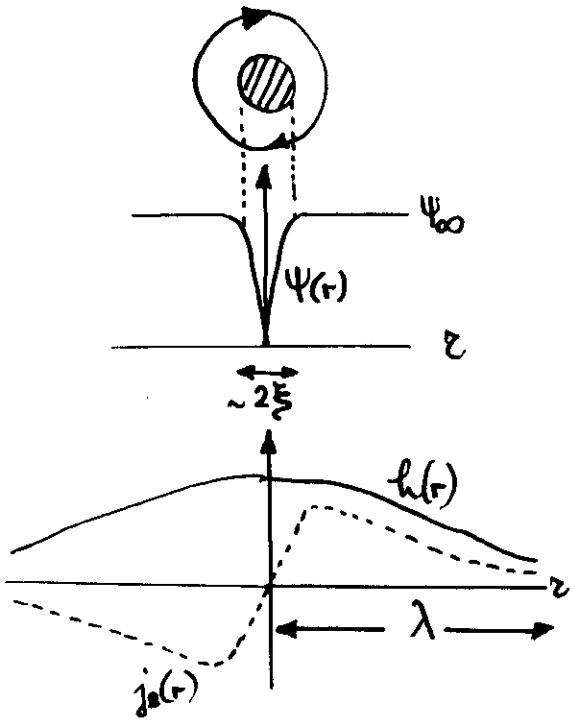

(ϕ flux quantum $= \frac{hc}{2e}$)

Limit $\varkappa \gg 1 \longrightarrow$ δ-function core

London eq.:

$$\lambda^2 \Delta \vec{h} - \vec{h} = \vec{\varphi}_0 \delta(\vec{r})$$

Solution:

$$h(r) = \frac{\varphi_0}{4\pi\lambda^2} K_0(r/\lambda$$

$\xi \ll r \ll \lambda$: $h(r) \sim \ln \frac{\lambda}{r}$

$r \gg \lambda$: $h(r) \sim e^{-r/\lambda}$

IV. TYPE I AND TYPE II SUPERCONDUCTORS

- SC AT "HIGH" MAGNETIC FIELD : FULL MEISSNER EFFECT (PERFECT DIAMAGNETISM) IS NO LONGER POSSIBLE

  ⟹ COEXISTENCE OF SC AND NORMAL REGIONS

- PROPERTIES OF A SC-N WALL : THE SURFACE ENERGY

$\xi \gg \lambda$

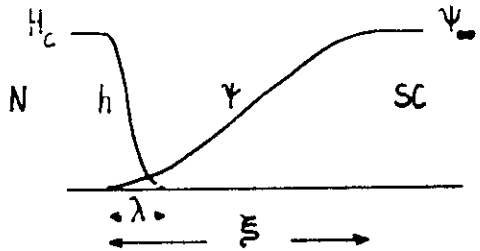

$\xi \ll \lambda$

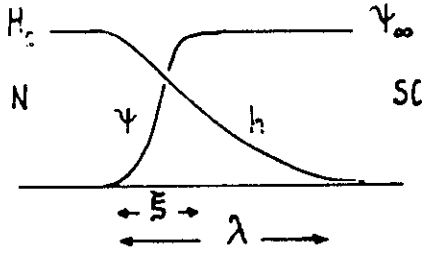

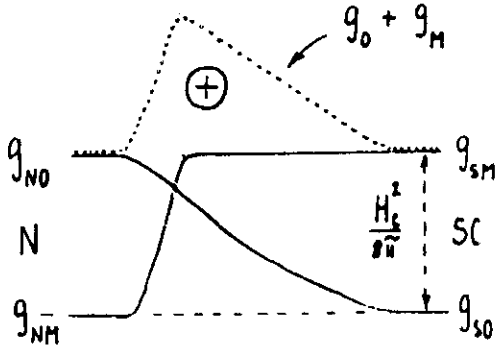

POSITIVE SURFACE ENERGY

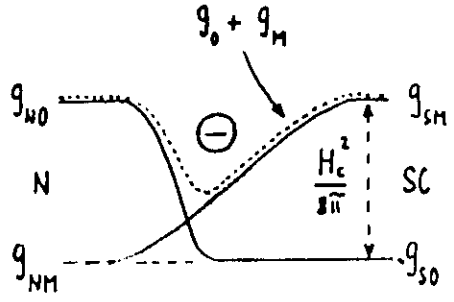

NEGATIVE SURFACE ENERGY

- ESTIMATE OF SURFACE ENERGY : $\sigma_{NS} \approx \frac{H_c^2}{8\pi}(\xi - \lambda)$

EXACT RESULT OF GL-THEORY :

GL-PARAMETER : $\underline{\kappa = \frac{\lambda}{\xi}}$

- $\kappa < \frac{1}{\sqrt{2}} \longrightarrow \sigma_{SN} > 0 \longrightarrow$ TYPE I SC
- $\kappa > \frac{1}{\sqrt{2}} \longrightarrow \sigma_{SN} < 0 \longrightarrow$ TYPE II SC

- TYPE I SUPERCONDUCTORS

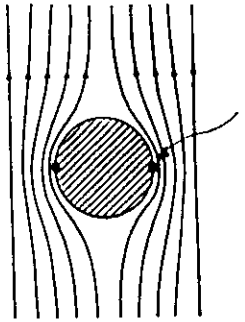

WHEN $H_{eq} = \frac{3}{2} H_\infty = H_c$

$\Rightarrow$ SC-PHASE BECOMES UNSTABLE

$\Rightarrow$ COEXISTENCE OF SC AND NORMAL REGIONS (INTERMEDIATE STATE) IN THE FIELD RANGE :

$$\frac{2}{3} H \leq H_\infty \leq H_c$$

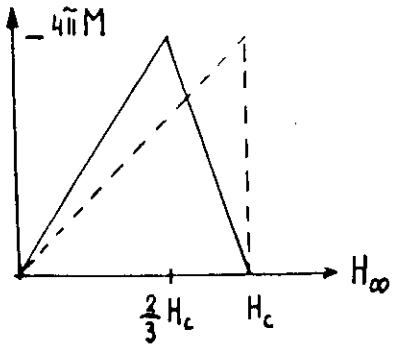

___ SC SPHERE --- LONG SC CYLINDER

- TYPE I SC : ALMOST ALL PURE SC ELEMENTS (EXCEPTIONS : NB AND V).

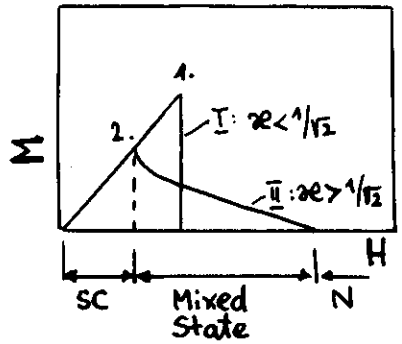

In ideal type II s.c. without defects : flux lines are moved by Lorentz forces

$$\vec{J}_c \times \vec{B} = -\vec{F}_p$$

J_c : critical current

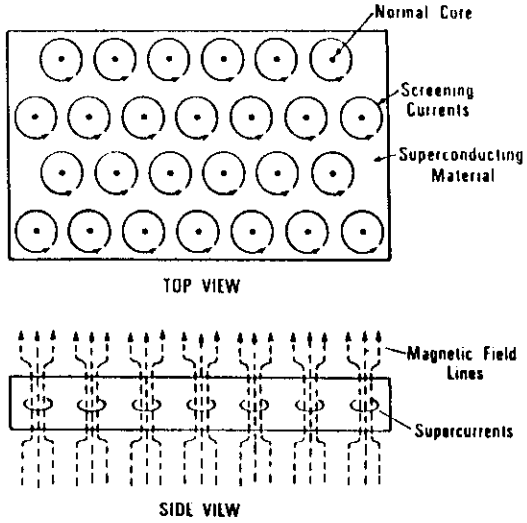

Figure 13.7 Representation of a vortex lattice in a Type II superconductor. The normal cores are represented by dots; the screening currents, by circles. The side view shows the distortion of an applied uniform magnetic field as it is channeled through each vortex core by the screening currents, leaving most of the superconducting material free of field.

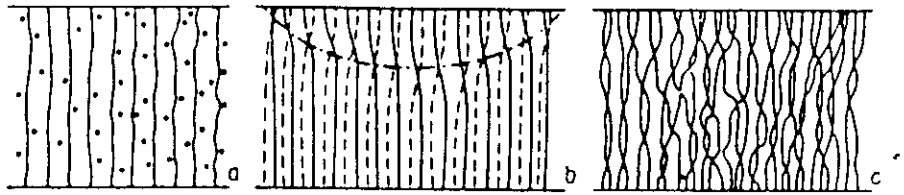

Figure 3: *Pinning of flux lines (solid and dashed lines) in a film in perpendicular magnetic field B_a. Schematic cross-sections. a) $B_a < B_{c_2}$: Small ratio of pinning strength to flux-line stiffness. Case of two-dimensional pinning. The dots indicate pins; these slightly curve the flux lines. b) $B_a = B_{c_2}$: A first screw dislocation nucleates at the surface and moves into the film (dash-dotted line). c) $B_a > B_{c_2}$: Many screw dislocations have penetrated. This highly disordered state is typical for the case of three-dimensional pinning. (Reproduced by permission from Brandt and Essmann [2]).*

The j - H - T Surface

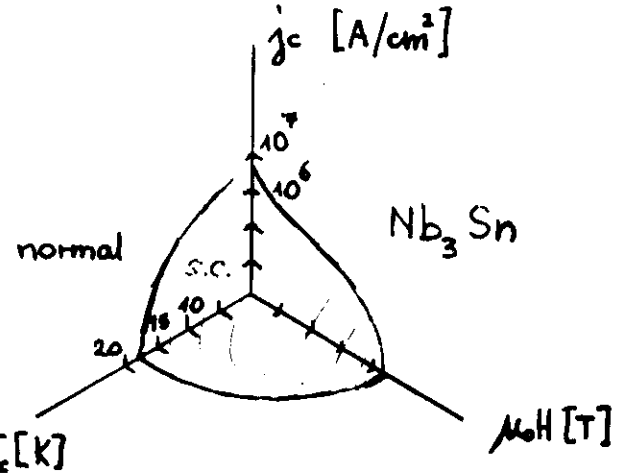

Type II superconductors in the mixed state:

j_c limited by flux motion

Lorentz Force on flux tubes:

$$\vec{F_L} = \vec{j} \times \vec{\Phi_0} = \vec{j} \times \vec{B}$$

Flux line movement dissipates energy → heating.

Velocity $\vec{v}$ of vortices → an electric field $\vec{E}$ is induced:

$$\vec{E} = n\vec{v} \times \vec{\Phi_0} = \vec{v} \times \vec{B}.$$

$\vec{E} \cdot \vec{j}$ = Power dissipation

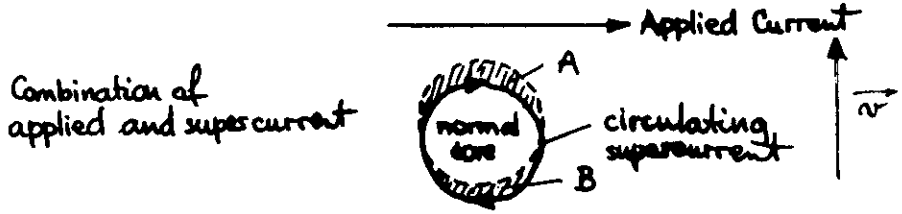

Condensation energy: $E = \frac{1}{2}\mu_0 H_c^2 \pi \xi^2$

Flux motion can be stopped by introducing metallurgical defects (energy is lowered):

- vacancies
- impurities
- voids
- dislocations
- grain boundaries
- twins

These defects "pin" the vortices in place.

→ PINNING CENTERS

Maximum pinning force (per flux tube)

$$\vec{f_p} = -(\vec{j_c} \times \vec{\Phi_0}) \quad :$$

Maximum pinning force (per unit volume):

$$\vec{F_p} = n\vec{f_p} = -(\vec{j_c} \times \vec{B})$$

no vali model summati

a) Point defects: Very small voids or particles of second phase, small clusters of other defects (f.ex. after irradiation)

b) Line defects: Dislocations, e.g. formed by cold working on ductile metals.

c) Surface defects : Grain boundaries, martensitic boundaries, twins, polymorphic transformations. (Main pinning source)

d) Volume defects : Large voids or precipitates. (In general not very effective as pinning sites)

EFFECT OF DEFECT SIZE

In classical superconductors, grain boundary pinning is the dominant mechanism.

→ The smaller the grains, the larger F_p, and thus j_c.

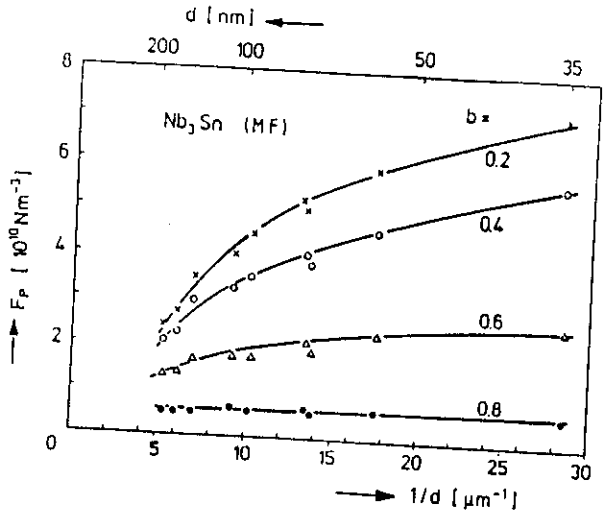

Figure 22. Volume pinning force as a function of the A15 grain size in Nb_3Sn wires (Schelb and Schauer, 1982).

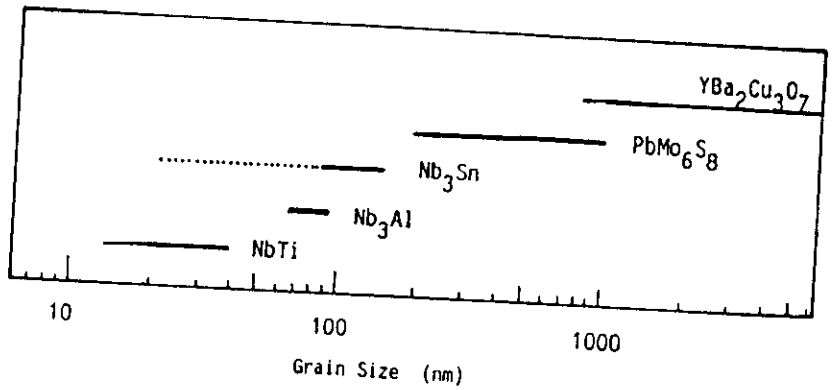

Figure 23. Average grain size range of various superconducting filamentary wires.

THE SIZE OF INCLUSIONS

Theory (Welch et al):

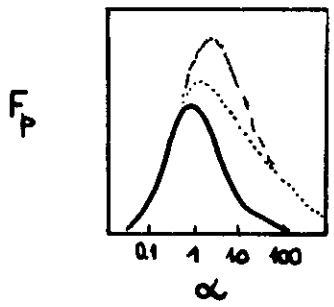

$\alpha = 0.882\, \xi_0 / \ell_e$

(impurity parameter)

$\longrightarrow$ $F_p(max)$ at $\alpha \approx 1$:

$$\xi_0 \approx \ell_e$$

$\longrightarrow$ Normal conducting inclusions should have a size and an interdistance comparable to ξ_0.

* This is the case for NbTi, where the normal conducting subbands produced by thermomechanical treatment have thicknesses of $\sim$ 10–20 nm.

* Enhanced pinning in Nb_3Sn by artificial Ta inclusions (Flükiger et al., 1987).

Measurement of J_c

a. Resistive (I-V) $\longrightarrow$ TRANSPORT CURRENTS (Intergrain)

b. Magnetization (Intragrain currents)

c. (a.c.) Induction Method (Campbell) $\longrightarrow$ Flux Profile
- J_c (Intragrain)
- J_c (Intergrain)

s.c. volume

J (Ind.) $\approx$ J_c (res.) Intragrain Currents

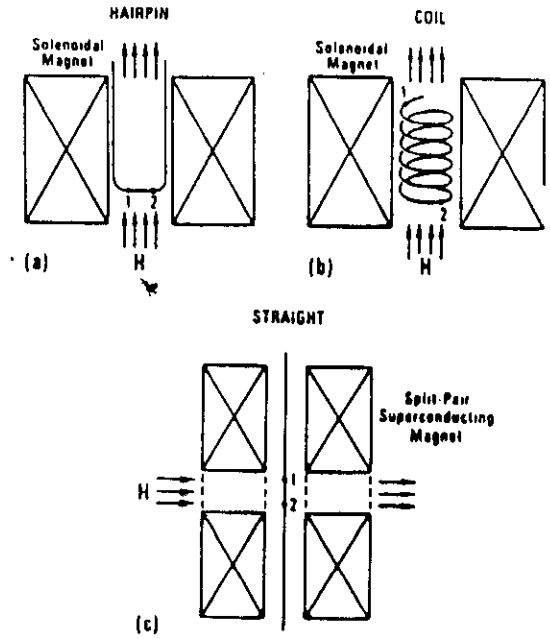

Experimental arrangements for determining short sample currents. Using a simple solenoidal magnet: (a) hairpin geometry and (b) coil sample geometry. Using a split coil: long, straight geometry. Voltage contacts are at points 1 and 2.

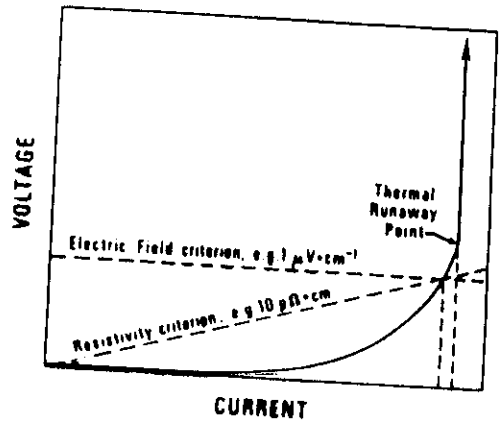

current-voltage characteristic of a practical superconductor with sition, electric field, and resistivity criteria for critical current rk and Ekin, 1977).

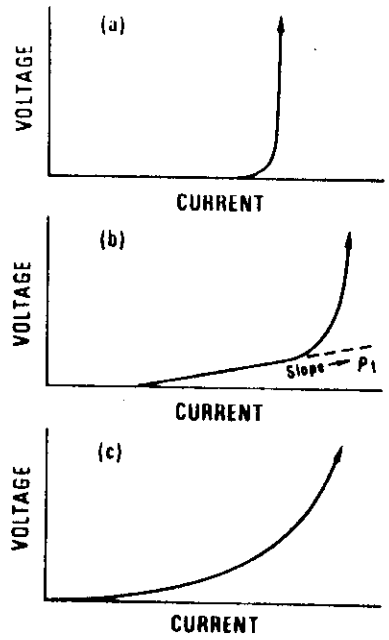

Figure G.1 Voltage–current characteristics for: (a) strong-pinning materials, (b) weak-pinning materials showing the superconducting flux flow region below J_c, and (c) damaged strong-pinning materials showing the nonlinear take-off region below J_c.

j_c BY MAGNETIZATION MEASUREMENTS

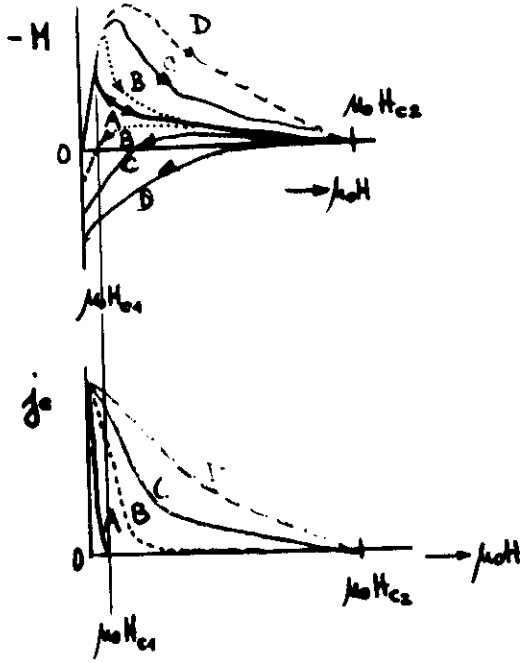

A: no flux pinning (reversible)

B: very weak pinni

C: irreversible, mod te flux pinnin

D: very irreversible strong flux pinn

Bean's model: $M_+ - M_- = a \cdot A \cdot j_c$

a ↑ radius

A ↑ geom. factor

For cylindrical grains:

$$\Delta M = 2 \cdot R \cdot \frac{1}{3} \cdot j_c$$

FLUX PROFILE MEASUREMENT of j_c

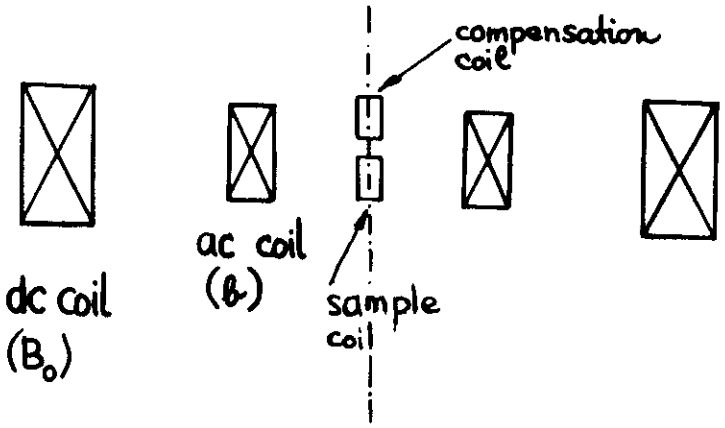

Flux change $d\Phi/dt$ induce a voltage U_s in the sample coil (pick-up coil). U_s is defined by the gradient dB/dx of the penetrated induction B (depending on B_0 and T).

If sample is in the <u>critical state</u>, the superposition of dc and ac field leads to a periodic change of the direction of dB/dx.

Critical state model

$$\frac{dB}{dx} = j_c$$

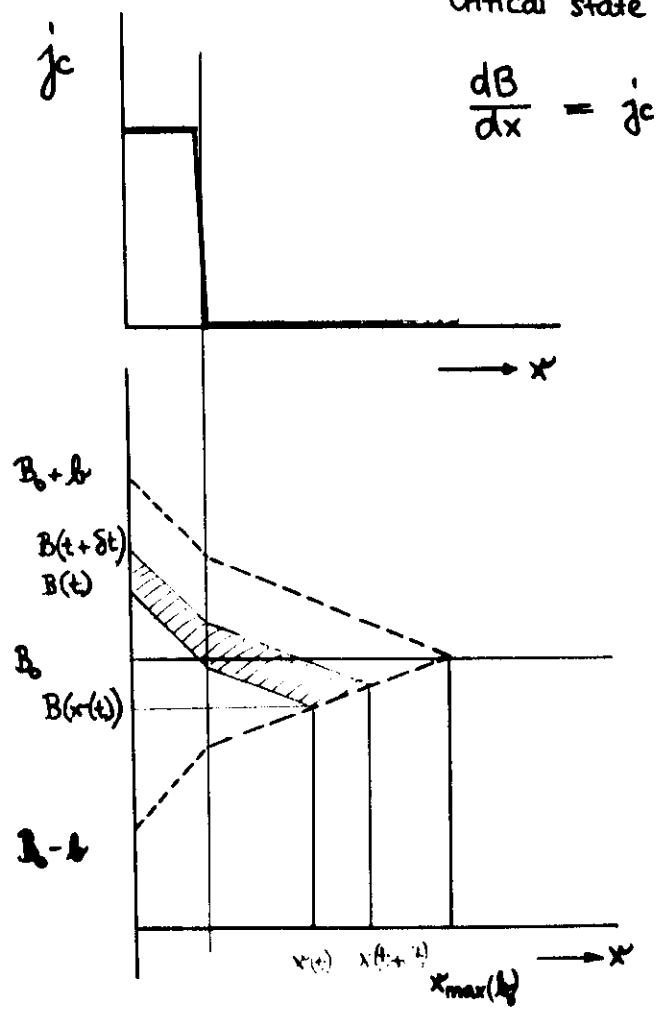

CRITICAL CURRENT DENSITY FLUX PROFILE MEASUREMENTS

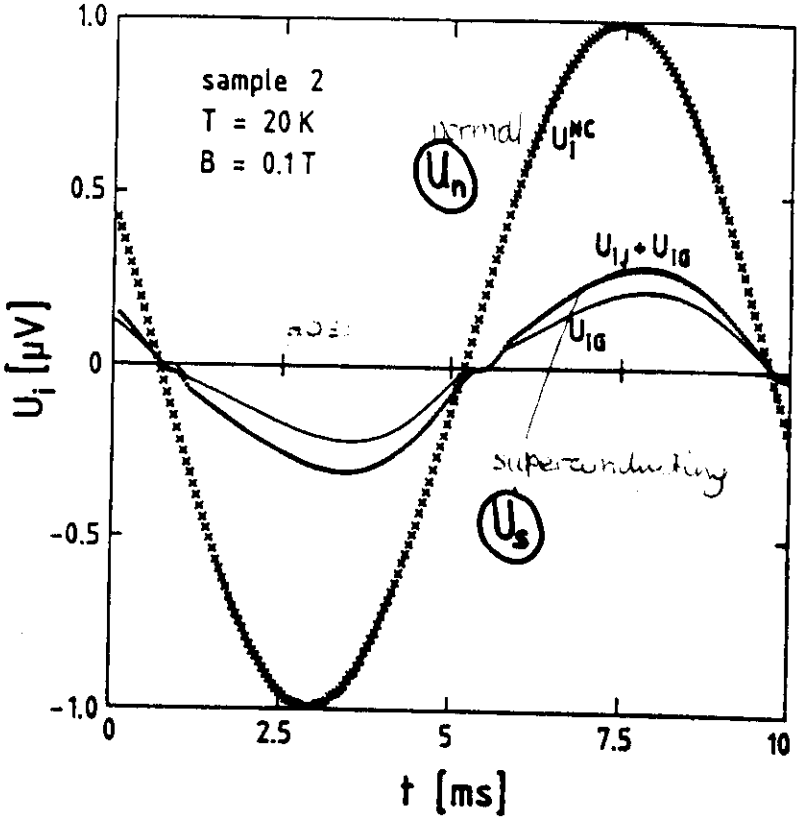

Calculation for a cylindrical sample (radius R):

$b = b_0 \cdot \sin(\omega t)$

$U_s = \bar{U}\,(R^2 - (x(t)-R)^2)\, b_0\, db/dt$

$U_n = \bar{U}\,(R^2)\, b_0\, db/dt$

with $\left.\frac{x(t)}{R}\right|_{normal} = 1$ and $\left.\frac{x(t)}{R}\right|_{supercond.} = 0$, it is

$$\frac{x(t)}{R} = 1 - \left(1 - \frac{U_s}{U_n}\right)^{0.5}$$

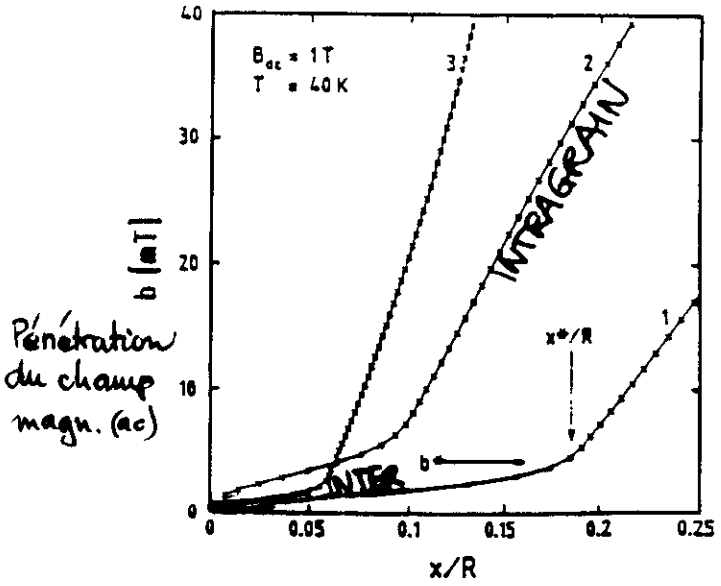

Pénétration du champ magn. (ac)

$$db/d(x/R) \sim J_c$$

(KÜPFER et al.)

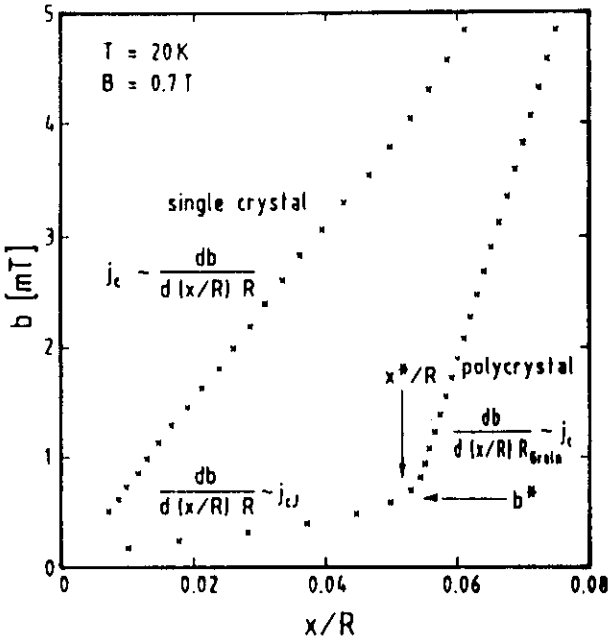

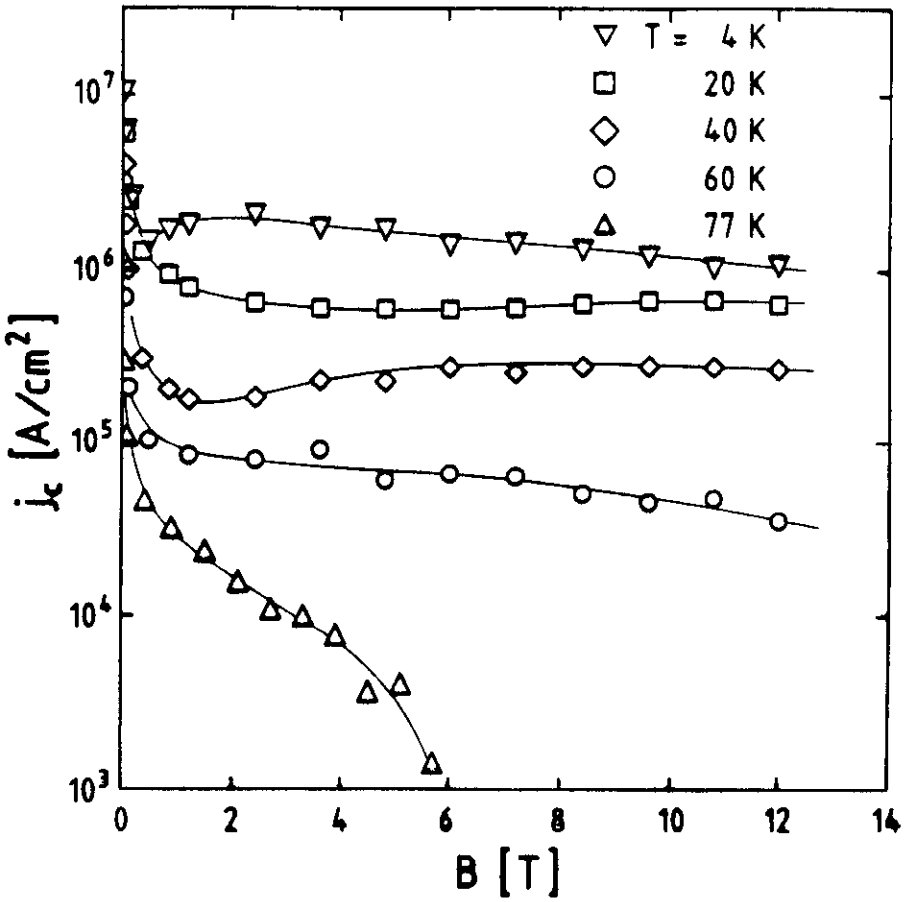

INTRAGRAIN J_c
(Eigenschaft der einzelnen Körner)

KÜPFER et al.

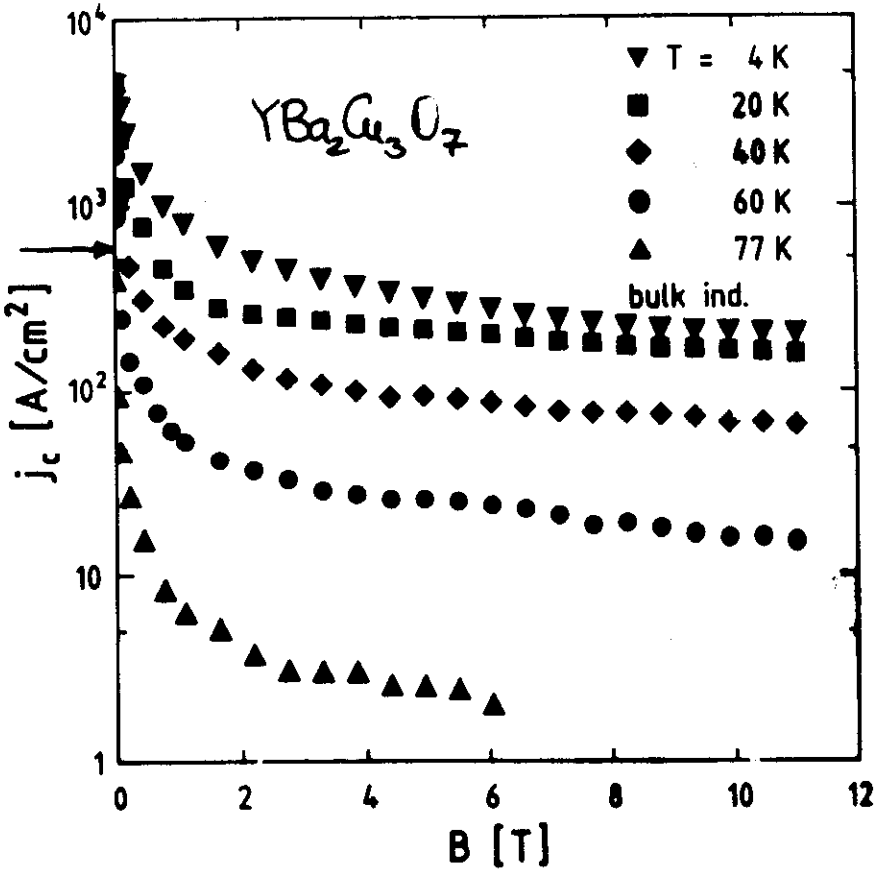

INTERGRAIN CRITICAL CURRENT DENSITY ~ RESISTIVE J_c